Polycyclic Aromatic Hydrocarbons Hot Paper

International Edition: DOI: 10.1002/anie.201912213
German Edition: DOI: 10.1002/ange.201912213

A Chiral Polycyclic Aromatic Hydrocarbon Monkey Saddle

*Tobias Kirschbaum, Frank Rominger, and Michael Mastalerz**

Abstract: *A contorted polycyclic aromatic hydrocarbon (PAH) in the shape of a monkey saddle has been synthesized in three steps from a readily available truxene precursor. The monkey saddle PAH is consisting of three five-, seven six-, and three eight-membered rings and has been unambiguously characterized by single-crystal X-ray diffraction. Owing to the three biaryl axes the monkey saddle PAH is inherently chiral. The inversion of the two enantiomeric structures into each other preferably occurs through a twisting of peripheral rings rather than by a fully planar intermediate, as has been calculated by DFT methods. Enantiomers were separated by chiral HPLC and inversion barriers determined by variable temperature circular dichroism spectroscopy, supporting the twisting mechanism.*

In recent years, the interest in structurally defined contorted polycyclic aromatic hydrocarbons (PAHs) has risen,[1] because they can be seen as models for defects in graphene, or, more interesting due to the intrinsic curvature as models to unusual three-dimensional carbon structures such as Mackay crystals.[2]

Curvature or contortion can be implemented into PAHs by the introduction of cove or fjord regions, even if the PAHs are consisting of six-membered rings exclusively.[1d,3] Another possibility is the embedding of rings that are deviating in size from the six-membered one, such as four-,[4] five-,[5] seven-,[5f,6] or eight-membered rings to cause contortion.[6b,7] With the exception of the four-membered ring containing PAH, the latter are by far the most rare ones.[1c–e]

Considering six-membered rings as "standard", there have also been combinations of different ring-sizes in one PAH, such as in the remarkable structure of a grossly warped nanographene with one pentagon and five heptagons,[8] or the large aromatic saddle of Miao and co-workers containing two heptagons and two pentagons.[9] Although the warped nanographene of the Itami group[8] or the twisted saddle based on an octagon from the Miao group[7d] are both chiral structures in the solid state as racemic crystals, the inversion barrier was too low to separate those at ambient conditions. To the best of our knowledge, no chiral negatively curved PAH based on multiple ring members deviating from "six" have been described to date; especially if one excludes those containing helical subunits or fjord regions.[10]

Herein, we report on a chiral negative curved PAH containing three eight- and three five-membered rings having the shape of a monkey saddle (Figure 1),[11] which is to the best of our knowledge unprecedented to date.

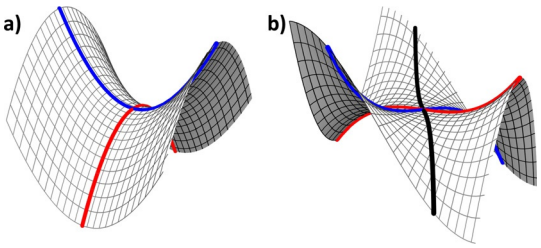

Figure 1. Comparison of horse saddle a) and monkey saddle b) according to the mathematical functions $f(x,y)=x^2-y^2$ (horse saddle) and $f(x,y)=x^3-3xy^2$ (monkey saddle). To illustrate the curvature two parabolas (red and blue) as well as three sigmoidals (blue, red, black) have been laid on the surfaces.

Key to the synthesis of the PAH monkey saddle is the realization of a threefold bromo-substitution at the aromatic benzene rings in the cove regions of truxene at the 4-,9-, and 14 positions.[12] To overcome any possible solubility issues, we synthesized truxene **1** with hexyloxy chains and brominated it with NBS in DMF, which selectively occurred *para* to the alkoxy chains in the cove regions at 4,9,14-positions of the truxene. Tribromotruxene **2** was isolated in 32 % yield besides tribromotruxene **3**, where one bromination occurred *ortho* to the alkoxy-chains (Scheme 1). Both structures have been elucidated by 2D NMR experiments (Supporting Information). At first glance, the observed selectivity is somewhat surprising, because unsubstituted truxenes preferably react at 2,7,12-positions in electrophilic aromatic substitutions[13] and

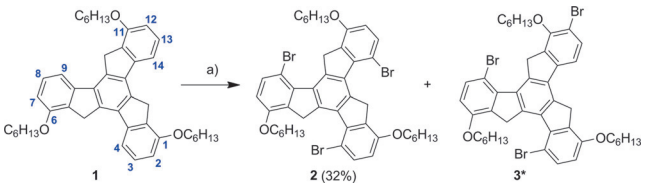

Scheme 1. Bromination of truxene **1**. a) NBS, DMF, RT, 18 h. *Only an analytical amount was purified to identify and fully characterize this compound, because on large scale it turned out to be difficult to completely remove further impurities. By adding a standard (trimethoxybenzene) to the crude product mixture a ratio of **3**:**2** has been identified with NMR yields of 48 % (**2**) and 38 % (**3**). For details see Supporting Information.

[*] M. Sc. T. Kirschbaum, Dr. F. Rominger, Prof. Dr. M. Mastalerz
Organisch-Chemisches Institut, Ruprecht-Karls-Universität Heidelberg
Im Neuenheimer Feld 270, 69120 Heidelberg (Germany)
E-mail: michael.mastalerz@oci.uni-heidelberg.de
Supporting information and the ORCID identification number(s) for the author(s) of this article can be found under: https://doi.org/10.1002/anie.201912213.

the alkoxy-substituents should enhance reactivity of these positions. However, DFT-calculations suggest that the transition state is according to the Hammond postulate close to the intermediate σ-complex, which is about 2.3 kJ mol^{-1} in favor of occurring in *para* position rather than in *ortho*-position (for details, see Supporting Information), thus overall a ratio of **2**:**3** of 55% to 31% is expected. Indeed, by adding trimethoxybenzene as a standard to the crude product mixture, NMR yields of 48% and 38% are determined, which are close to the calculated ratio by DFT.

Having tribromide **2** in hand, the next step of our approach is the threefold Suzuki–Miyaura cross-coupling with 2-formyl benzene boronic acid. Before doing so, we first tested the threefold cross-coupling reaction of **2** with 4-anisyl boronic acid under various conditions to find the best combination of palladium source and ligand, which turned out to be Pd_2dba_3 with *t*-Bu_3PHBF_4 and KF·2 H_2O, giving truxene **4** in 73% yield (Scheme 2). Applying the same conditions with 2-formylbenzene boronic acid gave truxene **5** in only 12% yield; here Pd_2dba_3 with XPhos and K_2CO_3 as base were the better choice and truxene **5** was isolated in 52% yield. Both structures were unambiguously characterized by single-crystal X-ray diffraction (see Supporting Information). The final step of the synthesis was the cyclization to the eight-membered rings by base-catalyzed condensation,[14] giving the monkey saddle PAH **6** in 55% yield. Monkey saddle **6** has been fully characterized (NMR, MS, IR, UV/Vis, elemental analysis). In the ^{1}H NMR the most characteristic peak is the singlet at $\delta = 8.36$ ppm, which can be assigned to the COT proton. Furthermore, a complex splitting of the signals for the two diastereotopic methylene protons directly attached to the oxygen can be observed, because of the intrinsic chirality of the molecule.

From DCM/MeOH high quality single-crystals suitable for X-ray diffraction were grown (Figure 2). PAH **6** crystallizes as racemate in the space group $C_{2/c}$ with two molecules of **6** and three additional dichloromethane molecules in the asymmetric unit (Figure 2c). The bonds of the six-membered rings are within the typical range of 1.38–1.41 Å, revealing benzenoid character (Figure 2b). The bonds of the five membered rings are with the exception of those shared with six-membered rings in the range of 1.47–1.49 Å and the bonds of the eight-membered rings are alternating between long and short ones. The shortest bonds here are between 1.331 and 1.347 Å (highlighted in blue) and found between the bridging methine and the carbon atom shared with the five-membered rings. The bonds that are the chiral biaryl axes are the longest ones (1.50 Å). The molecule is negatively curved with angles between unsubstituted peripheral benzene ring (highlighted in blue, Figure 2d,e) and the central ring (orange) of 40.6 to 52.9°. The angles between the hexyloxy substituted rings (green) and the central one are somewhat smaller (28.1 to 33.6°) and in the opposite direction. No pronounced π-stacking of the molecules is observed (Figure 2c), which explains the good solubility of the product.

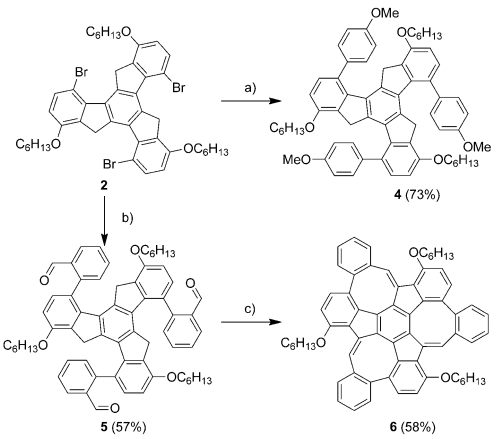

Scheme 2. Synthesis of monkey-saddle PAH **6**. a) 4-anisylboronic acid (9 equiv), 4 mol% Pd_2dba_3, 10 mol% *t*-Bu_3PHBF_4, KF·2 H_2O, THF, 60 °C, 20 h, 73%. b) (2-formylphenyl) boronic acid (6 equiv), 2 mol% Pd_2dba_3, 17 mol% XPhos, 2 M K_2CO_3, THF, 80 °C, 24 h, 57%. c) KOtBu, dry THF, 60 °C, 18 h, 58%.

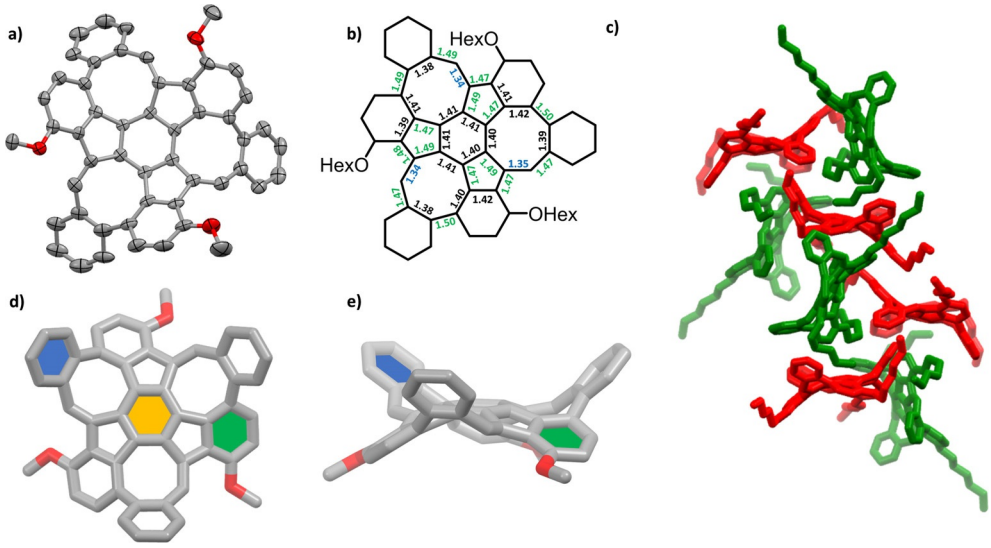

Figure 2. Single-crystal X-ray structure of monkey-saddle PAH **6**. a) One molecule as ORTEP drawing with probability of ellipsoids of 25%. b) Bond lengths of the core structure. Green: substantially longer than 1.40 Å; blue: substantially shorter than 1.40 Å. c) Packing of molecules, red: (S_a,S_a,S_a)-enantiomers; green: (R_a,R_a,R_a)-enantiomers. d) and e) Molecular structure with colored rings to highlight deviation from planarity as discussed in the main text. Depicted is only the (S_a,S_a,S_a)-enantiomers. In all presentations, hydrogens are omitted for clarity and in a), d) and e) only the first methylene carbon from the alkoxy chain is depicted.

Because the monkey saddle PAH is inherently chiral, we were interested if we can separate the enantiomers. The calculated inversion barrier for conversion of enantiomers via a planar C_{3h}-symmetric transition state is with 1813 kJ mol^{-1} extremely high to occur (Figure 3). More likely, other pathways such as partial twisting of the structure along single epimerizing atropisomeric axes give smaller barriers of 102 kJ mol^{-1}, but still too high to be detected by ^{1}H NMR spectroscopy: based on the Eyring equation, the expected coalescence temperature on the NMR time scale is 195 °C, which is too high to be observed with an ordinary NMR spectrometer in common deuterated solvents.

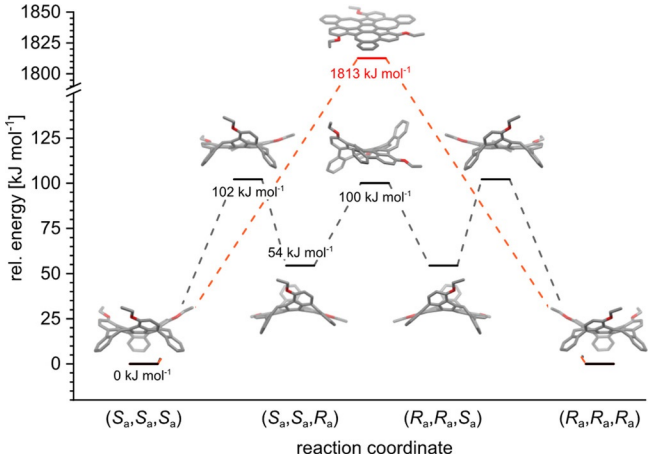

Figure 3. Calculated (B3LYP/6-311G(d,p)) activation barriers for the inversion of (R_a,R_a,R_a)-**6** to (S_a,S_a,S_a)-**6** via a planar transition state (red path) or partially twisted transition states (black path).

The calculated inversion barrier is comparable to that of 1,1-binaphtyl,[15] and therefore it is assumed that half-life ($\tau_{1/2}$) time at ambient temperature is large enough to separate the enantiomers.

Indeed, by applying a chiral HPLC column (Chiralpak IE^{TM} based on amylose *tris* (3,5-dichlorophenylcarbamate), the two enantiomers are separable by running an isocratic mixture of *n*-heptane/methyl-tert-butylether (MTBE) in the ratio of 80:20 at room temperature. Investigations of the separated compounds by circular dichroism spectroscopy in *n*-heptane/MTBE show that the spectra of the two enantiomers are mirror images with opposite Cotton effects (Figure 4). The most intense dissymmetry factor arises at 447 nm ($g_{abs} = 3.87 \times 10^{-3}$), which corresponds to the most bathochromic absorption maximum in the UV/Vis spectrum. A second maximum at 258 nm ($g_{abs} = 2.57 \times 10^{-3}$) with an inversed Cotton effect, fits to the most intense UV absorption at 278 nm. It is worth mentioning that these values are about the factor of 10 higher in chiroptical activity than for example, other chiral PAHs.[10c] To estimate the inversion barrier for the racemization, we measured its velocity by time-dependent CD spectroscopy at different temperatures (see also Supporting Information).[16] Using an Arrhenius plot (Supporting Information, Figure S72) the calculated inversion barrier is 104 ± 4 kJ mol^{-1} and fitting the one calculated by DFT (B3LYP/6-311G(d,p)) for the stepwise mechanism via twisted

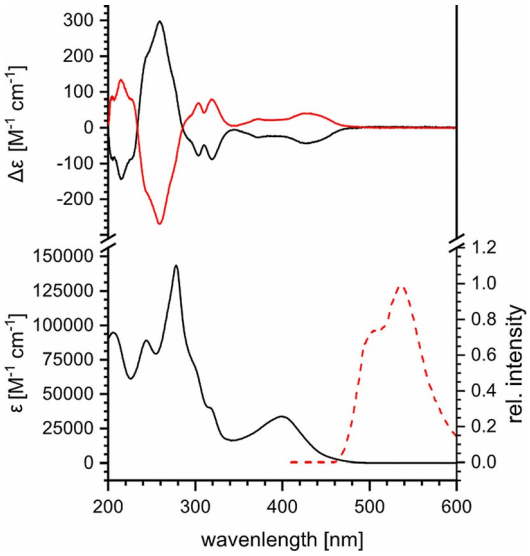

Figure 4. UV/Vis and fluorescence spectrum of racemic PAH **6** in *n*-heptane/MTBE (80:20) at room temperature (bottom) and CD spectrum of the separated enantiomers (top). Red: (R_a,R_a,R_a)-**6**; black:-(S_a,S_a,S_a)-**6**.

transition states (Figure 3). The half-life of **6** at room temperature is one day ($t_{1/2} = 23 \pm 1$ h). The mechanism for the inversion is similar as has been suggested for the larger [8]circulenes, although the Gibbs free energy for the inversion barriers are much lower (30.5 kJ mol^{-1} for tetrabenzo-[8]circulene and 38.5 kJ mol^{-1} for octabenzo-[8]circulene).[6b,7b] It is in a similar regime as calculated for the grossly warped nanographene by Scott, Itami, and coworkers (79.1 kJ mol^{-1}).[8] Unfortunately, no attempts for the separation of the enantiomers of this compound has been reported.

The energy levels of the frontier molecular orbitals of PAH **6** were calculated by DFT methods (B3LYP/6-311G-(d,p)). Owing to the intrinsic C_3-symmetry, there are two degenerated HOMO and LUMO levels each at $E_{HOMO} = -5.23$ eV and $E_{LUMO} = -1.90$ eV (Figure 5). For both HOMOs and LUMOs, the orbital lobes are distributed over the whole aromatic backbone. The energy gap between HOMOs and LUMOs is with $E_{g,DFT} = 3.33$ eV relatively large and significantly higher than estimated from the onset of the UV/Vis spectrum in dichloromethane (Figure 4). Herein, the gap is approx. $E_{g,opt} = 2.6$ eV. The absorption maxima are very broad and less structured with a most bathochromically shifted peak at $\lambda = 403$ nm. By TD-DFT calculations (see Supporting Information) this broad peak is a superposition of several transitions, namely HOMO to LUMO, HOMO to LUMO+1, and HOMO−1 to LUMO+1 at 432 nm; HOMO−2 to LUMO, HOMO−2 to LUMO−1 at 413 nm, and HOMO−1/HOMO to LUMO+2 at 362 nm. When irradiated at 403 nm, PAH **6** shows a broad emission with a peak maximum at 550 nm.

In conclusion, a monkey saddle shaped contorted and chiral PAH was synthesized in just three steps from a truxene precursor. The monkey saddle contains, besides six-membered rings, three five- and three eight-membered rings and

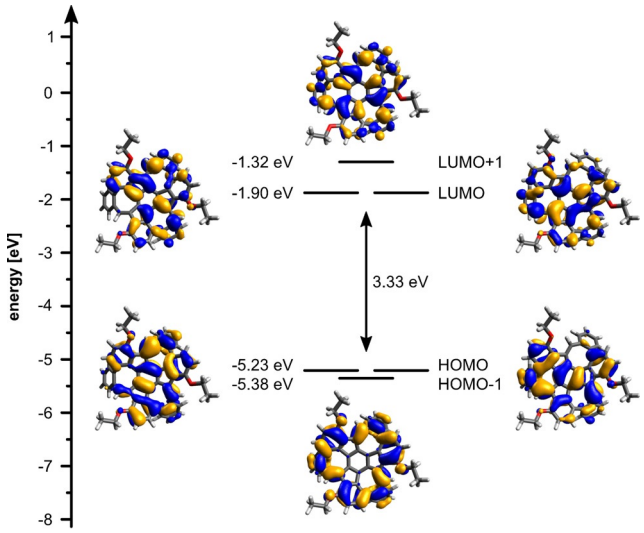

Figure 5. DFT calculations (B3LYP/6-311-G(d,p) of molecular orbitals of PAH **6**.

was studied by X-ray diffraction and other means. Owing to inherent chirality the synthesized racemic product was separated by chiral HPLC and the enantiomers were studied by CD spectroscopy. To our delight, the inversion barrier is with 102 kJ mol^{-1} high enough to handle the enantiopure monkey saddles at room temperature without racemization, which is, in our opinion, one necessary prerequisite to be able to achieve the synthetic goal of a fully conjugated sp^2-hybridized carbon based cage **7** (Figure 6), which contains "four" of the monkey saddle PAHs. It is worth mentioning that in the original paper of Mackay and Terrones, the curvature of the π-surface is based on the embedment of eight-membered rings,[2] as it is the case with PAH **6**. Currently, the synthetic challenge of cage compound **7** is tackled in our laboratory.

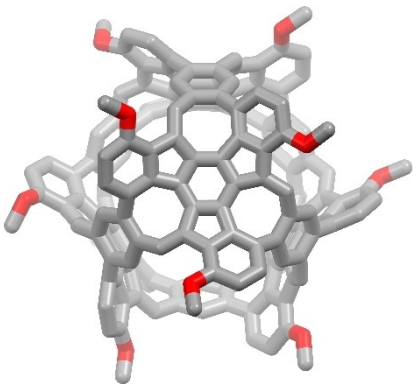

Figure 6. Geometry optimized model of a chiral fully conjugated cage compound **7** containing "four" monkey saddle units of PAH **6**.

Acknowledgements

The authors are grateful for funding this project (TP-A04) by Deutsche Forschungsgemeinschaft (DFG) within the collaborative research center SFB 1249 on "*N*-heteropolycycles as functional materials". Support by the state of Baden-Württemberg through bwHPC and the DFG through grant no INST 40/467-1 FUGG (JUSTUS cluster) is acknowledged.

Conflict of interest

The authors declare no conflict of interest.

Keywords: chirality · cyclooctatetraene · monkey saddle · negative curvature · truxene

How to cite: *Angew. Chem. Int. Ed.* **2020**, *59*, 270–274
Angew. Chem. **2020**, *132*, 276–280

[1] a) M. Rickhaus, M. Mayor, M. Juríček, *Chem. Soc. Rev.* **2017**, *46*, 1643–1660; b) S. H. Pun, Q. Miao, *Acc. Chem. Res.* **2018**, *51*, 1630–1642; c) Y. Segawa, H. Ito, K. Itami, *Nat. Rev. Mater.* **2016**, *1*, 15002; d) M. A. Majewski, M. Stępień, *Angew. Chem. Int. Ed.* **2019**, *58*, 86–116; *Angew. Chem.* **2019**, *131*, 90–122; e) I. R. Márquez, S. Castro-Fernández, A. Millán, A. G. Campaña, *Chem. Commun.* **2018**, *54*, 6705–6718.

[2] A. L. Mackay, H. Terrones, *Nature* **1991**, *352*, 762.

[3] For examples, see: a) K. Baumgärtner, A. L. M. Chincha, A. Dreuw, F. Rominger, M. Mastalerz, *Angew. Chem. Int. Ed.* **2016**, *55*, 15594–15598; *Angew. Chem.* **2016**, *128*, 15823–15827; b) M. Ball, Y. Zhong, Y. Wu, C. Schenck, F. Ng, M. Steigerwald, S. Xiao, C. Nuckolls, *Acc. Chem. Res.* **2015**, *48*, 267–276.

[4] R. B. Bharat, T. Bally, A. Valente, M. K. Cyrański, Ł. Dobrzycki, S. M. Spain, P. Rempała, M. R. Chin, B. T. King, *Angew. Chem. Int. Ed.* **2010**, *49*, 399–402; *Angew. Chem.* **2010**, *122*, 409–412.

[5] a) V. M. Tsefrikas, L. T. Scott, *Chem. Rev.* **2006**, *106*, 4868–4884; b) Y.-T. Wu, J. S. Siegel, *Chem. Rev.* **2006**, *106*, 4843–4867; c) A. Sygula, P. W. Rabideau, *J. Am. Chem. Soc.* **2000**, *122*, 6323–6324; d) M.-K. Chen, H.-J. Hsin, T.-C. Wu, B.-Y. Kang, Y.-W. Lee, M.-Y. Kuo, Y.-T. Wu, *Chem. Eur. J.* **2014**, *20*, 598–608; e) T.-C. Wu, M.-K. Chen, Y.-W. Lee, M.-Y. Kuo, Y.-T. Wu, *Angew. Chem. Int. Ed.* **2013**, *52*, 1289–1293; *Angew. Chem.* **2013**, *125*, 1327–1331; f) K. Shoyama, F. Würthner, *J. Am. Chem. Soc.* **2019**, *141*, 13008–13012.

[6] a) S. H. Pun, C. K. Chan, J. Luo, Z. Liu, Q. Miao, *Angew. Chem. Int. Ed.* **2018**, *57*, 1581–1586; *Angew. Chem.* **2018**, *130*, 1597–1602; b) S. H. Pun, Y. Wang, M. Chu, C. K. Chan, Y. Li, Z. Liu, Q. Miao, *J. Am. Chem. Soc.* **2019**, *141*, 9680–9686; c) K. Yamamoto, T. Harada, M. Nakazaki, T. Naka, Y. Kai, S. Harada, N. Kasai, *J. Am. Chem. Soc.* **1983**, *105*, 7171–7172; d) K. Yamamoto, T. Harada, Y. Okamoto, H. Chikamatsu, M. Nakazaki, Y. Kai, T. Nakao, M. Tanaka, S. Harada, N. Kasai, *J. Am. Chem. Soc.* **1988**, *110*, 3578–3584; e) M. Sato, K. Yamamoto, H. Sonobe, K. Yano, H. Matsubara, H. Fujita, T. Sugimoto, K. Yamamoto, *J. Chem. Soc. Perkin Trans. 2* **1998**, 1909–1914; f) X. Gu, H. Li, B. Shan, Z. Liu, Q. Miao, *Org. Lett.* **2017**, *19*, 2246–2249; g) J. M. Farrell, V. Grande, D. Schmidt, F. Würthner, *Angew. Chem. Int. Ed.* **2019**, https://doi.org/10.1002/anie.201909975; *Angew. Chem.* **2019**, https://doi.org/10.1002/ange.201909975.

[7] a) C.-N. Feng, M.-Y. Kuo, Y.-T. Wu, *Angew. Chem. Int. Ed.* **2013**, *52*, 7791–7794; *Angew. Chem.* **2013**, *125*, 7945–7948; b) Y. Sakamoto, T. Suzuki, *J. Am. Chem. Soc.* **2013**, *135*, 14074–14077; c) R. W. Miller, A. K. Duncan, S. T. Schneebeli, D. L. Gray, A. C. Whalley, *Chem. Eur. J.* **2014**, *20*, 3705–3711; d) K. Y. Cheung, C. K. Chan, Z. Liu, Q. Miao, *Angew. Chem. Int. Ed.* **2017**, *56*, 9003–9007; *Angew. Chem.* **2017**, *129*, 9131–9135; e) H. Chen, Q. Miao, *ChemPlusChem* **2019**, *84*, 627–629; f) S. Nobusue, K. Fujita, Y. Tobe, *Org. Lett.* **2017**, *19*, 3227–3230;

g) J.-X. Chen, J.-W. Han, H. N. C. Wong, *Org. Lett.* **2015**, *17*, 4296 – 4299; h) K. Y. Cheung, S. Yang, Q. Miao, *Org. Chem. Front.* **2017**, *4*, 699 – 703; i) A. Rajca, A. Safranov, S. Rajca, R. Shoemaker, *Angew. Chem. Int. Ed. Engl.* **1997**, *36*, 488 – 491; *Angew. Chem.* **1997**, *109*, 504 – 507.

[8] K. Kawasumi, Q. Zhang, Y. Segawa, L. T. Scott, K. Itami, *Nat. Chem.* **2013**, *5*, 739.

[9] K. Y. Cheung, X. Xu, Q. Miao, *J. Am. Chem. Soc.* **2015**, *137*, 3910 – 3914.

[10] a) C. M. Cruz, I. R. Márquez, I. F. A. Mariz, V. Blanco, C. Sánchez-Sánchez, J. M. Sobrado, J. A. Martín-Gago, J. M. Cuerva, E. Maçôas, A. G. Campaña, *Chem. Sci.* **2018**, *9*, 3917 – 3924; b) C. M. Cruz, S. Castro-Fernández, E. Maçôas, J. M. Cuerva, A. G. Campaña, *Angew. Chem. Int. Ed.* **2018**, *57*, 14782 – 14786; *Angew. Chem.* **2018**, *130*, 14998 – 15002; c) C. M. Cruz, I. R. Márquez, S. Castro-Fernández, J. M. Cuerva, E. Maçôas, A. G. Campaña, *Angew. Chem. Int. Ed.* **2019**, *58*, 8068 – 8072; *Angew. Chem.* **2019**, *131*, 8152 – 8156.

[11] T. E. Cecil, P. J. Ryan, *Am. Math. Month.* **1986**, *93*, 380 – 382.

[12] To the best of our knowledge, 4,9,14-tribromotruxene by trimerization of the corresponding 7-bromo indanone was reported before by Echavarren and co-workers: R. Dorel, P. de Mendoza, P. Calleja, S. Pascual, E. González-Cantalapiedra, N. Cabello, A. M. Echavarren, *Eur. J. Org. Chem.* **2016**, 3171 – 3176; However, unfortunately neither a protocol, nor yields or analytical data were given.

[13] B. Gómez-Lor, Ó. de Frutos, P. A. Ceballos, T. Granier, A. M. Echavarren, *Eur. J. Org. Chem.* **2001**, 2107 – 2114.

[14] a) G. Zhang, F. Rominger, M. Mastalerz, *Chem. Eur. J.* **2016**, *22*, 3084 – 3093; b) G. Zhang, F. Rominger, U. Zschieschang, H. Klauk, M. Mastalerz, *Chem. Eur. J.* **2016**, *22*, 14840 – 14845.

[15] L. Meca, D. Řeha, Z. Havlas, *J. Org. Chem.* **2003**, *68*, 5677 – 5680.

[16] M. Rickhaus, L. Jundt, M. Mayor, *Chimia* **2016**, *70*, 192 – 202.

[17] CCDC 1954747 (**1**), 1954748 (**4**), 1954749 (**5**), and 1954750 (**6**) contains the supplementary crystallographic data for this paper. These data are provided free of charge by The Cambridge Crystallographic Data Centre.

Manuscript received: September 24, 2019
Revised manuscript received: October 14, 2019
Accepted manuscript online: October 15, 2019
Version of record online: November 18, 2019

